EPJ Web of Conferences **293**, 00048 (2024) https://doi.org/10.1051/epjconf/202429300048
mm Universe 2023

Impact of filaments on galaxy cluster properties in The Three Hundred simulation

S. Santoni[1,*], M. De Petris[1], A. Ferragamo[1], G. Yepes[2], and W. Cui[2,3]

[1]Dipartimento di Fisica, Sapienza Università di Roma, Piazzale Aldo Moro 5, I-00185 Rome, Italy
[2]Departamento de Fısica Teorica & CIAFF, Facultad de Ciencias, Universidad Autonoma de Madrid, Modulo 8, E-28049 Madrid, Spain
[3]Institute for Astronomy, University of Edinburgh, Edinburgh EH9 3HJ, UK

Abstract. Galaxy clusters and their filamentary outskirts reveal useful laboratories to test cosmological models and investigate Universe composition and evolution. Their environment, in particular the filaments of the Cosmic Web to which they are connected, plays an important role in shaping the properties of galaxy clusters. In this project, we analyse the gas filamentary structures present in 324 regions of The Three Hundred hydrodynamical simulation extracted with the DisPerSE filament finder. We estimate the number of gas filaments globally connected to several galaxy clusters, i.e. the connectivity k, with a mass range of $10^{13} \leq M_{200}\, h^{-1}\, M_{\odot} \leq 10^{15}$ at redshift $z = 0$. We study the positive correlation between the connectivity and mass of galaxy clusters. Moreover, we explore the impact of filaments on the dynamical state of clusters, quantified by the degree of relaxation parameter χ.

1 Introduction

Clusters of galaxies, the largest gravitationally bound systems in the Universe, reside at the nodes of the Cosmic Web [1] and are connected by a multitude of filamentary structures. In the outskirts of the clusters, matter and galaxies are funneled towards the centre through filaments. A comprehensive knowledge of the filaments connected to galaxy clusters is essential to understand the influence of the environment on galaxy cluster properties and evolution. One way to quantify the filamentary skeleton around the cluster is through the so-called connectivity k [2], defined as the number of filaments globally connected to the galaxy cluster, estimated at a specific aperture. This project aims to investigate the impact of filaments on the main galaxy cluster properties, in particular in this work we focus on their masses and dynamical state.

2 The Three Hundred project

In this work, we analyse the multiple zoom-in regions of The Three Hundred hydrodynamical simulation [3]. The Three Hundred project[1] aims to model 324 regions whose volumes have cubic side lengths of $30\, h^{-1}\, Mpc$, centered on massive galaxy clusters, with a mass

*e-mail: sara.santoni@uniroma1.it
[1]https://the300-project.org

$M_{200} > 6.42 \times 10^{14}\, h^{-1}\, M_{\odot}$. The Three Hundred regions are re-simulated with higher resolution from 324 regions of the $1\, h^{-1}\, Gpc$ Dark Matter-only MDPL2 MultiDark [4] simulation, centered on the most massive galaxy clusters at $z = 0$. The cosmological parameters used in the MDPL2 and The Three Hundred simulations are those measured by the *Planck* mission [5]. The regions have been re-simulated with different baryonic models: Gadget-MUSIC [6], Gadget-X [7], which is used in this work, and more recently Gizmo-Simba [8]. For each region, 128 snapshots are available from redshift $z = 17$ to $z = 0$. The simulated regions were analysed using the AHF halo finder [9] which self-consistently includes both gas and stars in the halo finding process. The halo finder extracts haloes and estimates their properties, such as the radius R_{Δ}[2], mass M_{Δ} and density profile.

3 Methods

3.1 Cosmic Web extraction

The gas particle distribution of The Three Hundred regions are analysed with DisPerSE [10], a topological structure finder, designed to extract the structures of the Cosmic Web. The finder identifies topologically significant features in the input density field, which is obtained through a Delaunay tesselation in the case of a 2D or 3D discrete distribution. The noise introduced by the finite sampling of the distribution is quantified and reduced with the persistence and topological simplification theories. The persistence parameter, which quantifies the robustness of a topological pair, is defined as the difference of the values of the critical points in the pair and is used to filter low significant filaments. As an output, DisPerSE provides the positions of the extreme points found in the distribution: maxima, minima, saddle points and bifurcation points, where a filament splits in two. The filaments are given as a set of segments connecting a maximum and a saddle point.
For our analysis, we first binned the gas particle distribution of each region at redshift $z = 0$ in a three-dimensional grid of $30\, h^{-1}\, Mpc$ per side, and within each region we give a pixel resolution of $150\, h^{-1}\, kpc$. Then, to avoid sharp variations from one pixel to another, we applied a Gaussian smoothing with a σ of 4 pixels. Finally we applied an absolute persistence cut of 0.2, to focus on significant filaments connecting clusters and haloes. The node distribution extracted from DisPerSE was compared with the AHF halo catalogue of each region, to match the DisPerSE maximum points to the simulated haloes and clusters. To avoid a possible low-resolution contamination near the borders, we consider only the haloes inside a sphere of $13\, h^{-1}\, Mpc$ radius from the centre of each region. The final data set includes 3×10^3 haloes and clusters with a mass range from $10^{13} \leq M_{200}\, h^{-1}\, M_{\odot} \leq 5 \times 10^{15}$.
The gas skeleton extracted from The Three Hundred simulated regions is a good tracer of the overall matter distribution and accretion to galaxy clusters. In particular, throughout the 324 simulated regions there is a good spatial agreement between the gas filaments and both the Dark Matter and mock galaxy filaments, both from 3D and 2D extractions [11, 12].

3.2 Connectivity measurements

For each halo we estimated the connectivity k, which is defined in [2] as the number of filaments globally connected to a cluster. Different definitions are used in literature to estimate this parameter. In this work, we compute the connectivity as the number of filaments crossing a specific spherical surface at a radius R_{Δ} from the centre of the cluster. In particular,

[2]The subscript Δ indicates the overdensity, i.e. value of the ratio between the density of the cluster at that radius and the critical density of the Universe $\rho_c = 3H^2/(8\pi G)$ at the cluster's redshift.

we estimate the connectivity at R_{200} and at R_{500}, defined respectively as k_{200} and k_{500}. With this definition, we are taking into consideration also the filaments that are coming from substructures and bifurcation points that lie within the sphere, which contribute to the cluster's properties and therefore also to its connectivity.

4 Results

In this work we investigate if the number of filaments connected to a cluster, quantified by the connectivity, is correlated with the main properties of the cluster itself, mainly its mass and dynamical state.

4.1 Connectivity and galaxy cluster mass

The number of filaments connected to a cluster is expected to correlate with the mass of the cluster itself, as many studies show [13–16]. The expected trend is for the connectivity to increase with the mass of the cluster.
Taking the advantage to investigate a cluster's sample with the largest mass range, we analyse the connectivity of a set of groups and clusters extracted from The Three Hundred simulation at redshift $z = 0$. Figure 1 shows the values of the connectivity k_{200} as a function of the clusters mass M_{200}. We measured the mean and the standard deviation for each mass bin, chosen by taking into account the overall mass distribution in The Three Hundred simulation at $z = 0$, shown in the bottom panel of the figure. We performed a linear fitting, whose parameters are shown in Table 1, as the following: $\log k_{200} = A \cdot \log M_{200} + B$.

Table 1. The fitted parameters for the $\log k_{200} - \log M_{200}$ relation.

	$\log k_{200} - \log M_{200}$
A	0.298 ± 0.016
B	-3.78 ± 0.23

We compare our estimates of the connectivity to similar measurements from literature studies, as shown in Figure 2. We compare our sample both to simulated, as [13], and observed data, such as [14–16]. The trend of the connectivity with the mass is well in agreement, within the errors, with the ones from literature, despite the differences presented in Table 2, and over a larger mass range. More specifically, the connectivity is estimated at a fixed aperture in [13, 14], while the connectivity from our work and [15, 16] is estimated at an overdensity radius. Other differences can arise from the Cosmic Web component chosen to extract the filamentary skeletons, such as gas, Dark Matter or galaxies particles and from the different filament finder used in the analyses. We refer to [13–16] for a more detailed description of the datasets used.

Table 2. A summary of the parameters of previous studies compared to this work.

	Data	k_R	M	CW extraction
The300	Hydro simulation	R_{200}	M_{200}	3D gas particles
AC+10 [13]	DM simulation	3 Mpc	M_{Vir}	3D DM particles
S+19 [14]	Observations	1.5 Mpc	M_{200}	2D galaxies
DF+19 [15]	Observations	1.5 R_{Vir}	M_{200}	2D galaxies
M+20 [16]	Observations (Coma Cl.)	R_{Vir}	M_{200}	3D z-slice galaxies

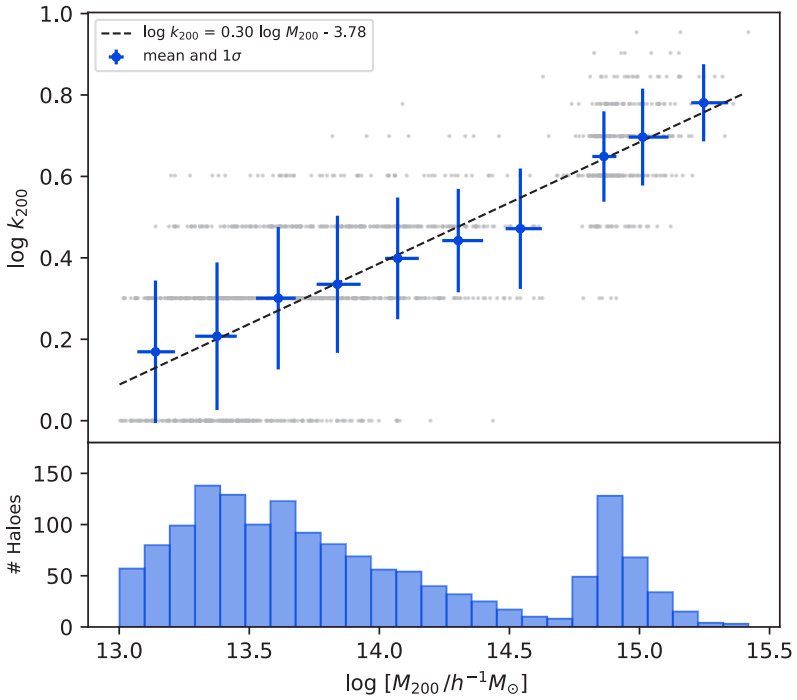

Figure 1. The connectivity of groups and clusters $\log k_{200}$ plotted as a function of the mass $\log(M_{200}/h^{-1}M_{\odot})$ (grey points). In the top panel the mean and standard deviation values are also plotted. The bottom panel shows the mass distribution of groups and clusters of The Three Hundred hydrodynamical simulation at redshift $z = 0$ analysed in this work.

4.2 Connectivity and galaxy cluster dynamical state

In this subsection we investigate the correlation between the connectivity and the dynamical state of The Three Hundred clusters. We quantify the dynamical state with the degree of relaxation χ, as defined by [17]:

$$\chi_{\Delta} = \left(\frac{(\frac{f_s}{0.1})^2 + (\frac{\Delta_r}{0.04})^2 + (\frac{|1-\eta|}{0.15})^2}{3} \right)^{-1/2}$$

where f_s is the sub-halo mass fraction, Δ_r is the centre-of-mass offset and η is the virial ratio. The threshold values for these parameters were chosen following [18]. A cluster is considered as dynamically relaxed when $\chi \geq 1$. To study the effect of connectivity on the dynamical state of clusters, independently on their masses, we divide the data set in three different connectivity and mass sub-samples. Respectively, we consider weakly connected ($k_{200} < 4$), medium connected ($k_{200} = 4$) and highly connected ($k_{200} > 4$) clusters along with low mass ($M_{200} < 7 \times 10^{13}\, h^{-1}M_{\odot}$), medium ($7 \times 10^{13} \leq M_{200}\, h^{-1}M_{\odot} < 5.5 \times 10^{14}$) and massive ($M_{200} \geq 5.5 \times 10^{14}\, h^{-1}M_{\odot}$) clusters.

In the left and right panels of Figure 3 we display the degree of relaxation as a function of the mass and connectivity, respectively, for three connectivity and mass bins. At a fixed mass, the left panel of Figure 3 shows that there is no evident correlation between connectivity

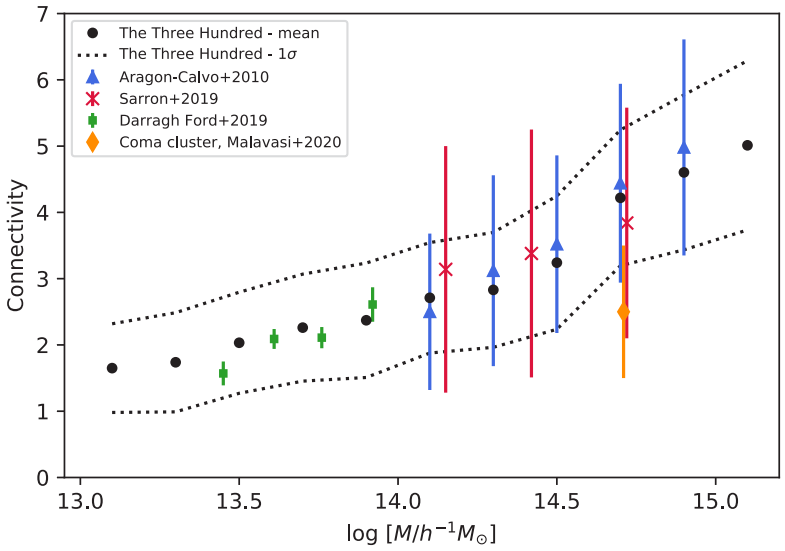

Figure 2. Connectivity of The Three Hundred clusters, compared with literature values. For each work, we plot the mean values of the connectivity. The error bars refer to the standard deviation values for this work, [13, 14, 16], while for [15] they represent the errors on the mean values.

and the degree of relaxation, as the three sub-samples overlap. On the other hand, at fixed connectivity, the right panel of the figure shows a slight correlation between the mass and χ, indicating that less massive haloes are on average more dynamically relaxed. This result is in disagreement with that found by [19], where at fixed mass, weakly connected clusters are on average more relaxed than highly connected clusters. These differences may depend on the different data set and Cosmic Web extraction analysed in their work, to which we refer the reader for more details.

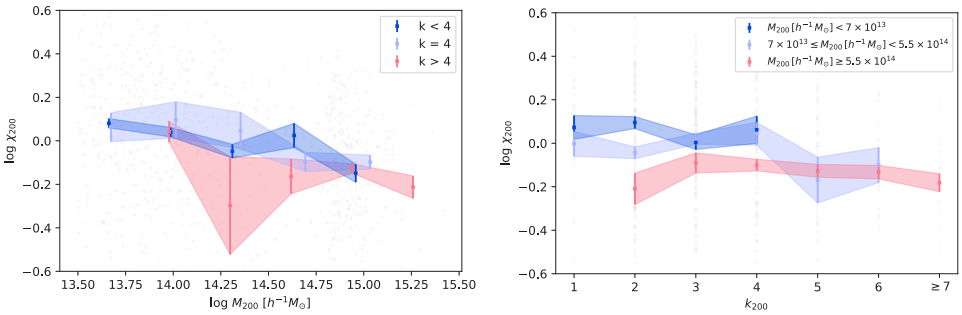

Figure 3. *Left panel*: mean degree of relaxation as a function of the mass M_{200} for three connectivity k_{200} bins ($k < 4$, $k = 4$ and $k > 4$). *Right panel*: mean degree of relaxation as a function of the connectivity k_{200} for three mass M_{200} bins. In both panels, the errors bars represent the errors on the mean values.

5 Conclusions

In this work we analysed the gas filamentary structures connected to The Three Hundred hydrodynamical simulation clusters and their impact on galaxy cluster properties. We extracted the gas skeletons at $z = 0$ with the DisPerSE filament finder in the 324 regions of the simulation and we estimated the connectivity k_{200} of groups and clusters.
The main conclusions of this work can be summarized in the following:

1. The connectivity is correlated with the mass of haloes and clusters, with more massive clusters being on average more connected. This result is compatible with previous results from literature, both from simulations and observations;

2. We do not find a correlation between the connectivity and the dynamical state of clusters, quantified in terms of the degree of relaxation χ.

References

[1] Bond J. R. *et al.*, Nature **380**, 603 (1996)
[2] Codis S. *et al.*, Monthly Notices of the Royal Astronomical Society **479**, 973 (2018)
[3] Cui W. *et al.*, Monthly Notices of the Royal Astronomical Society **480**, 2898 (2018)
[4] Klypin A. *et al.*, Monthly Notices of the Royal Astronomical Society **457**, 4340 (2016)
[5] Planck Collaboration *et al.*, Astronomy and Astrophysics **594**, A13 (2016)
[6] Sembolini F. *et al.*, Monthly Notices of the Royal Astronomical Society **429**, 323 (2013)
[7] Rasia E. *et al.*, The Astrophysical Journal **813**, L17 (2015)
[8] Cui W. *et al.*, Monthly Notices of the Royal Astronomical Society **514**, 977 (2022)
[9] Knollmann S. R. *et al.*, Astrophysics Source Code Library (2011)
[10] Sousbie T., Monthly Notices of the Royal Astronomical Society **414**, 350 (2011)
[11] Kuchner U. *et al.*, Monthly Notices of the Royal Astronomical Society **494**, 5473 (2020)
[12] Kuchner U. *et al.*, Monthly Notices of the Royal Astronomical Society **503**, 2065 (2021)
[13] Aragón-Calvo M. A. *et al.*, Monthly Notices of the Royal Astronomical Society **408**, 2163 (2010)
[14] Sarron F. *et al.*, Astronomy and Astrophysics **632**, A49 (2019)
[15] Darragh Ford E. *et al.*, Monthly Notices of the Royal Astronomical Society **489**, 5695 (2019)
[16] Malavasi N. *et al.*, Astronomy and Astrophysics **634**, A30 (2020)
[17] Haggar R. *et al.*, Monthly Notices of the Royal Astronomical Society **492**, 6074 (2020)
[18] Cui W. *et al.*, Monthly Notices of the Royal Astronomical Society **464**, 2502 (2017)
[19] Gouin C. *et al.*, Astronomy and Astrophysics **651**, A56 (2021)